Journal of Energetic Materials
Publication details, including instructions for authors and subscription information:
http://www.informaworld.com/smpp/title~content=t713770432

Thermolysis of various energetic substances by exposure to adiabatically compressed gas

R. L. Piunti[a]; K. R. Brower[a]
[a] Department of Chemistry, New Mexico Institute of Mining and Technology, Socorro, New Mexico

To cite this Article Piunti, R. L. and Brower, K. R.(1995) 'Thermolysis of various energetic substances by exposure to adiabatically compressed gas', Journal of Energetic Materials, 13: 1, 107 — 139
To link to this Article: DOI: 10.1080/07370659508019346
URL: http://dx.doi.org/10.1080/07370659508019346

THERMOLYSIS OF VARIOUS ENERGETIC SUBSTANCES BY EXPOSURE TO ADIABATICALLY COMPRESSED GAS

R.L. Piunti and K.R. Brower

Department of Chemistry

New Mexico Institute of Mining and Technology

Socorro, New Mexico 87801

Abstract: A transient thermal stimulus of 0.1 to 5.0 ms duration is delivered to the surface of a solid or liquid test substance by adiabatic compression and reexpansion of an inert gas. Pressures in the low kilobar range and temperatures up to 3000 K are readily accessible. The quantity of heat transferred is governed by the peak internal energy density, θ, of the gas. Chemical reaction begins abruptly at a minimum threshold value of θ. The reaction products can be identified and quantized by FTIR spectrometry and GC/MS chromatography.

Tests on various chemical classes of energetic materials showed that each class (nitrate esters, nitramines, nitroarenes and benzenediazonium salts) has nearly a common threshold which correlates with the energy of the weakest bond.

The condensed residue resulting from pyrolysis of the energetic materials was analyzed by GC/MS and several mechanisms of decomposition have been proposed.

Some features of the heat transport process were investigated by use of chemically stable high-melting compounds which are converted from angular grains to spheroidal beads by melting. The amount of heat transferred from the gas to a solid particle is proportional to the surface area and the peak temperature is inversely proportional to the heat capacity which is proportional to the volume. Grains equal to or smaller

Journal of Energetic Materials Vol. 13, 107-139 (1995)
Published in 1995 by Dowden, Brodman & Devine, Inc.

than a certain size are melted. By interpolation , it is possible to predict approximately what value of internal energy density of the compressed gas will heat a particle to a given temperature.

INTRODUCTION

During pyrolysis by adiabatic compression, an inert gas is heated reversibly to a temperature up to several thousand degrees at pressures up to one kilobar in accordance with the adiabatic gas law,

(1) $$T = T_o\ (V_o/V)^{\gamma - 1}$$ where

γ = ratio of heat capacities at constant pressure and volume and,

V_o/V = compression ratio.

A thermal pulse, which is found experimentally to be determined by the rate of compression and the peak internal energy density,

(2) $$\theta = (C_V/R)\,P_o(V_o/V)^{\gamma}$$

is delivered to an energetic substance by conduction from hot compressed gas. The duration of the thermal pulse for a specified compression ratio is proportional to the square root of the impacting mass which compresses the gas.

Bowden and Gurton[1] were among the first to study energetic substances using adiabatic compression primarily to investigate the causes of accidental explosions. Their objective was to correlate the compressed air temperature with the temperature calculated for air for reactions in 10^{-5} seconds.

Evans and Yuill[2] used adiabatically compressed O_2 , air, N_2, and Ar to find the minimum gas temperature required for incipient ignition of nitroglycerin and PETN. For a given compression ratio, Ar was found to be more efficient than N_2 in causing ignition. On the other hand, at a given gas

temperature, N_2, was found to be more efficient than Ar. Argon has lower values of thermal conductivity, heat capacity and density. As a result, there is less efficient heat transfer from gas to condensed phase. Oxygen was found to be more efficient than N_2 in causing ignition, indicating that the chemical nature of the gas in contact with the energetic substance is also important.

Freedman[3] has studied the difficult problem of thermal ignition of energetic substances. The difficulty lies in the non-linear dependence of heat evolution rate on temperature. Because of the non-linear temperature dependence, exact explicit solutions for the critical conditions and time to explosion have been unattainable. Freedman was able to solve the thermal ignition problem by using approximate algebraic equations instead of non-linear differential equations, but his results were not accurate when steep temperature gradients existed at the point of ignition.

Earlier, Rice[4] had investigated heat conduction during thermal gaseous explosions. His conclusion was that at lower pressures, conduction and not convection was important. For convection, Taylor[5] had recognized that a molten layer separates solid explosive from the gas phase reactions.

Hicks[6] appears to have defined the problem of heat transport very clearly. The ordinary differential equations governing heat transport are non-linear because the reaction rate depends on the factor, exp (-E/RT). The process of ignition is a transition from an unreactive state to one of self-sustaining combustion so that a steady state is not attained. Thus for thermal ignition, the temperature is a function of position as well as time and an exact thermal ignition theory must involve solutions of non-linear partial differential equations.

The problem of heat transport is even more difficult for adiabatic

compression because of changing thermal conductivity, heat capacity and density. Pasman[7] appears to have achieved some success using approximations and lengthy iterative procedures. The cylinder containing the gas is divided into eight parallel layers and an equal amount of heat is released at the midplanes. From this construction, an approximate expression is obtained for the desired quantity which is the surface layer temperature. However, that expression also contains the heat flux at the surface. The heat flux at the surface is not obtainable, but Pasman surmounts the problem by setting the heat flux at the surface equal to a quantity which is obtainable, the heat flux due to the chemical decomposition.

Most recently, Brower[8] has investigated the heat transport problem in a direct and chemically useful fashion. His idea was to correlate the surface layer temperature to the temperature of the Arrhenius equation. In this study, we present some results which substantiate this idea along with useful relationships between surface layer temperature, internal energy density, and type of gas to be adiabatically compressed. In addition, the above variables have been related to a relatively recent additional variable, also introduced by Brower, the exposure or reaction time. His method for finding the reaction time is to measure the width of an oscilloscope trace obtained from the piston displacement and light intensity resulting from a pyrolysis. Each point of the oscilloscope recording of piston displacement as a function of time represents a value of the compression ratio, V_o/V, where

(3) V_o = volume of the cylinder cavity containing the gas at time, t=0 , and

V = volume of the cylinder cavity containing compressed gas

at time, t.

Each value of the compression ratio has an associated temperature, T, as given by (1). The time-temperature history and activation energy for the reaction in question give the effective reaction time[9].

We have found that the yield of pyrolysis products resulting from adiabatic compression is proportional to the initial pressure of the gas when V_o/V is maintained constant and also proportional to the temperature of the gas when the initial pressure is constant. The yield of products therefore appears to be determined by the available internal thermal energy density, (2), which can be defined as,

(4) $\theta = (nC_v/V)(T - T_o) = (C_vP/RT)(T - T_o) = \{P_o(V/V_o)^\gamma\}\{C_v(T - T_o)\}/RT$

$= \{P_o(V/V_o)^\gamma\}\{C_v(1 - T_o/T)\}/R.$

In most cases , $T>>T_o$.

In order to determine the reaction threshold, we have constructed plots of the yield of a characteristic product versus the internal energy density and extrapolated to zero yield of product. For each of the classes of compounds investigated, which includes the benzenediazonium salts, the nitrate esters, the nitramines and the nitroaromatics, it was found that the threshold was correlated to the energy of the weakest bond initially severed in the thermal decomposition pathway. Such plots also indicate how the percent decomposition varies with the thermal pulse delivered. For insensitive compounds, the percent decomposition is expected to remain relatively low for severe thermal pulses corresponding to high values of θ . The upward curvature of these plots is due to exothermic secondary reactions such as the rapid, exothermic reduction of oxides of nitrogen. It is expected that plots of product yield versus internal energy density will not be the same for different reaction times. Those products

which are rapidly consumed will appear in decreasing amounts at longer reaction times. On the other hand, products formed in subsequent pathways will only appear at the longer reaction times or in very small amounts at shorter reaction times. To find whether a product is consumed at all, we have plotted the yield of that product versus the extent of reaction as measured from the amount of CO_2 and CO generated. A decrease of the amount of product, often plotted as mL product/mL CO_x versus the extent of reaction, mL CO_x indicates that the product is being consumed.

The products used for the construction of the plots previously described are gases resulting from pyrolysis and include CH_4, CO_2, CO, HCN, C_2H_2, C_2H_4, N_2O, NO and NO_2. Many of the energetic compounds pyrolyzed to obtain those gases have good or, at least, fair oxygen balance and as a result fail to give identifiable condensed phase products. However, monofunctional compounds which are not explosives but which belong in the same chemical class as the energetic compounds of interest are expected to provide identifiable condensed phase products of pyrolysis. The monofunctional nitrate esters, nitramines and nitroaromatics should pyrolyze according to the same mechanism as the polyfunctional compounds. Therefore it is worth the effort to analyze condensed phase products resulting from pyrolysis of the analogs with poor oxygen balance since we can often deduce a mechanism which will then apply to the oxygen rich analogs as well. The mechanism of decomposition can vary, however, with the number of functionalities. A well known example is the pyrolysis of TNT which gives coke as product in contrast to the oxygen-poor analog, nitrobenzene, which gives clean products.

DISCUSSION

Heat Transport

The salts were melted by the adiabatic compression method as described in the experimental section. From our results, the following trends were observed.

(A) At constant θ and exposure time , the diameter (x) of the largest melted spheroidal bead decreases as the number of internal degrees of freedom of the adiabatically compressed gas increases.

(B) For any of the adiabatically compressed gases, the diameter of the largest melted spheroidal bead decreases with decreasing exposure time at constant θ.

(C) For any of the adiabatically compressed gases, the diameter of the largest melted spheroidal bead decreases as the melting temperature increases at constant exposure time and θ.

(D) At constant melting temperature , exposure time. and melted grain size , the required value of θ is greater for those adiabatically compressed gases having more internal degrees of freedom.

(E) At constant melting temperature and melted grain size, the rate of change of θ with exposure time is greater for those adiabatically compressed gases having fewer degrees of freedom.

(F) For any of the adiabatically compressed gases, the rate of change of θ with exposure time is greater at higher temperatures

In an individual experiment , the quantity of heat , ΔH , crossing unit area of substrate , will remain approximately constant for particles of different sizes because the dose of heat is limited by diffusion through the gas according to the equation,

(5) $$d^2 = 2 D t ,$$

where D is the thermal diffusivity of the gas. The magnitude of ΔH can be estimated by multiplying the molar density , molar heat capacity , temperature rise , and depth , d , in the gas . The temperature rise in the substrate particle is nearly uniform because its thermal conductivity is much greater than that of the gas . The temperature rise is given by ,

(6) $\Delta T =$ (area of particle) $\Delta H/($ heat capacity per cm^3) .

The temperature rise is greater for particles of smaller size , x , since the heat capacity per cm^3 of such particles is less . It follows from (6) that ,

(7) $\Delta T = (nx^2\Delta H)/(\rho c_p x^3) = (n\Delta H)/(\rho c_p x)$,

where n = shape factor (n=6 for a cube exposed on all sides)

ρ = density of the particle

c_p = specific heat.

It should also be mentioned that the temperature rise of the substrate is related to exposure time through the rate of compression. We would not expect an extremely slow compression to give the same heating effect as a rapid compression because of dissipation losses . The effect becomes significant somewhere near the one-millisecond range of effective reaction time .

The experimental values of melted particle size were extrapolated to 10 micrometers and the corresponding values of θ tabulated as shown in Table 1. The extrapolation to a 10-micrometer particle with convergent heating was chosen because the typical yield of reaction products from a liquid substrate of non-energetic material, with θ well above the threshold, is roughly stoichiometrically equivalent to a 5-micrometer layer with unidirectional heating.

Table 1

p (bar)	Exposure time (μs)	Gas
T, 611°K		
250	100	Ar
295	350	Ar
500	1500	Ar
420	100	N_2
440	350	N_2
590	1500	N_2
500	100	CO_2
520	350	CO_2
520	1500	CO_2
1072	100	CH_4
1075	350	CH_4
1100	1500	CH_4
T, 867.8°K		
320	100	Ar
490	350	Ar
800	1500	Ar
510	100	N_2
595	350	N_2
810	1500	N_2
1000	100	CO_2
1075	350	CO_2
1140	1500	CO_2
T, 1073°K		
410	100	Ar
530	350	Ar
1200	1500	Ar
600	100	N_2
810	350	N_2
1320	1500	N_2

Table 2

T (K)	Equation Giving θ (bar)*
Ar	
611	0.179 t + 232
867.8	0.374 t + 286
1073	0.564 t + 353
N_2	
611	0.121 t + 408
867.8	0.214 t + 489
1073	0.514 t + 549
CO_2	
611	0.0857 t + 491
867.8	0.100 t + 990
CH_4	
611	0.0200 t + 1070

*Valid for exposure times, t, between 100 and 1500 μS

We wanted to substantiate the idea that a value of θ which melts a particle of 10-micrometer size and heats a 5-micrometer layer of substrate of equal volumetric heat capacity, would, in fact, impart the temperature, T_m . It was realized that the value of ΔH is independent of substrate. We show later in the section dealing with the benzenediazonium salts and also at the end of the present section, that a value of θ for the onset of pyrolysis of ArN_2^+ or $R\text{-}ONO_2$ or $ArNO_2$, gives an estimated temperature in agreement with the temperature obtained for kt=1 according to the Arrhenius law for the reaction in question.

The extrapolated θ values of Table 1 can be plotted versus exposure time. However, the plots will be straight lines for which equations are readily obtained and presented in the second column of Table 2 . Each of the equations has the form y = m x + b, where y = θ and x = exposure time for the respective surface layer temperatures listed in the first column of the table. Using these equations, θ can be immediately obtained at any exposure time between 100 and 1500μs for any of the three surface layer temperatures using any of the gases listed.

The pyrolysis of nitrobenzene conducted in N_2 under adiabatic compression at 100 μs reaction time was found to give a threshold of 600 bar by plotting the mL of NO_x evolved during the pyrolysis versus the corresponding values of the internal energy density. From Table 2 it is apparent that the third equation listed under N_2 also gives a value of 600 bar for θ at 100 μs. The temperature corresponding to the third equation is 1073 K (the melting point of NaCl) and it is that melting point of 1073 K which should equal the Arrhenius equation temperature using the appropriate pre-exponential factor and activation energy for the pyrolysis

of nitrobenzene. The Arrhenius equation for the pyrolysis of nitrobenzene is ,

(8) $$C_6H_5NO_2 \rightarrow C_6H_5\cdot + NO_2\cdot$$

$$k\,(s^{-1}) = 1.90 \times 10^{15}\, e^{-33026\,T},$$

so that for a reaction time of 100 μs , T is equal to 1273 K which agrees reasonably well with the estimate.

Residue Analysis

The residue resulting from pyrolysis of N-nitropiperidine, N-nitropyrrolidine, β-nitrostyrene, cyclohexanol nitrate, and orthonitrotoluene gave ion chromatograms which identified such products as pyridine, pyrrole, styrene, hexanal, benzene and toluene. The respective decomposition mechanisms are presented in Schemes 1 to 5.

The pyrolysis of orthonitrotoluene (Scheme 5) gave a residue which appeared to contain benzene and toluene. In order to rule out any adventitious source, deuterated orthonitrotoluene was pyrolyzed under conditions identical for the pyrolysis of orthonitrotoluene and d_6-benzene and d_8-toluene were attained. The decomposition mechanism to produce toluene must involve initial formation of a radical as in step 1 of Scheme 5, followed by elimination of nitrite ion and reduction to toluene as given in steps 2 and 3[10]. No precedent for the formation of benzene appears to be known.

Benzenediazonium Salts

The FTIR spectra of the gaseous pyrolysis products of benzenediazonium fluoroborate revealed absorbance peaks at 1603, 1500, 1238 and 754 cm^{-1} due to fluorobenzene. The production of fluorobenzene shows that the Schiemann mechanism remains viable at very high

Scheme 1

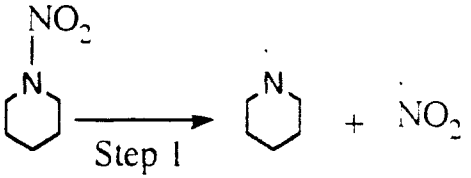

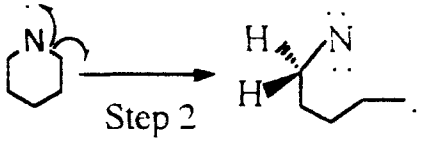

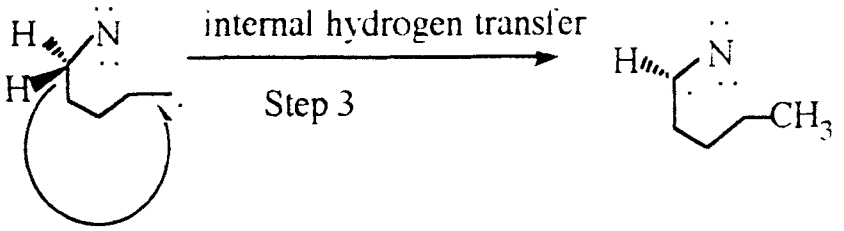

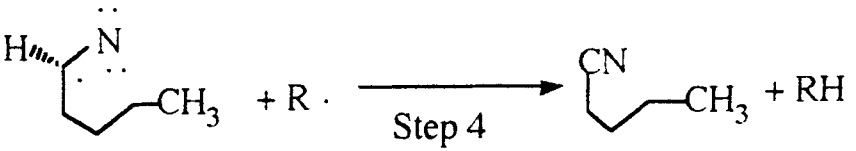

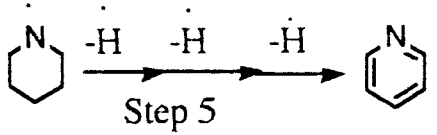

Scheme 2

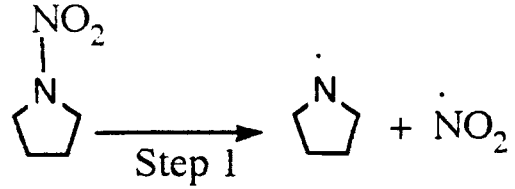

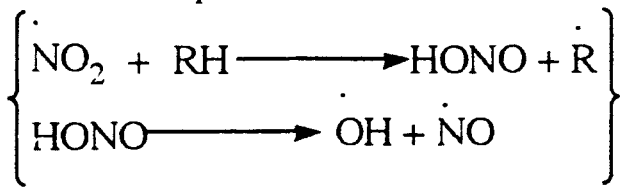

Step 2

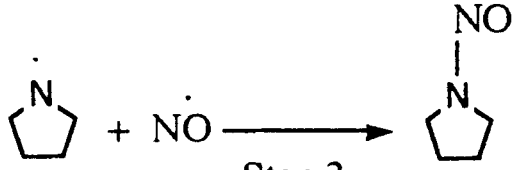

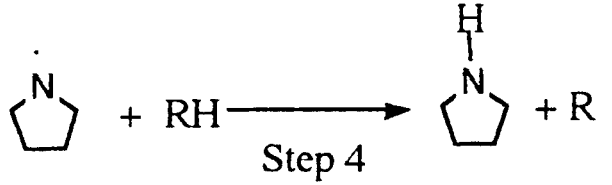

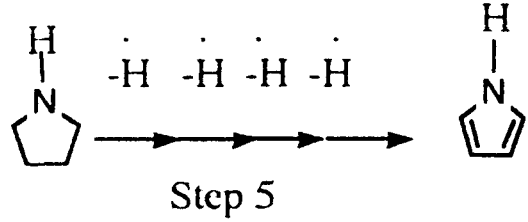

Scheme 3

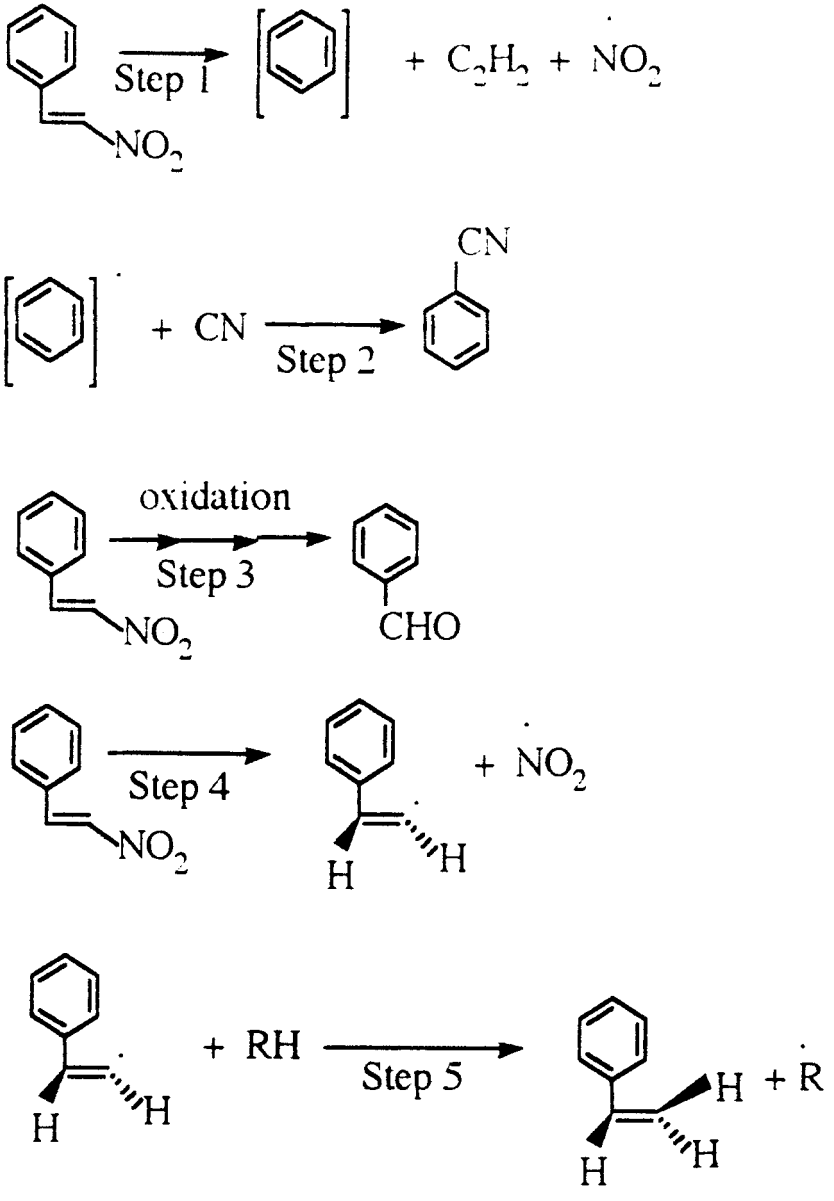

Scheme 4

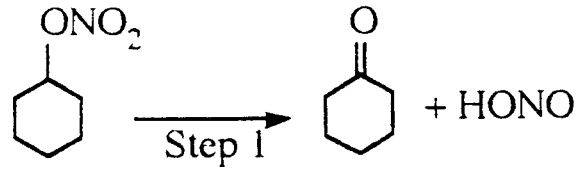

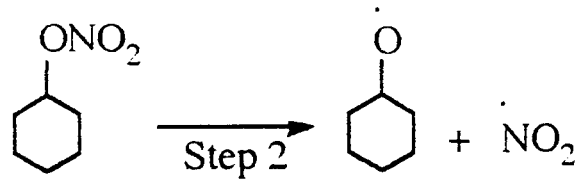

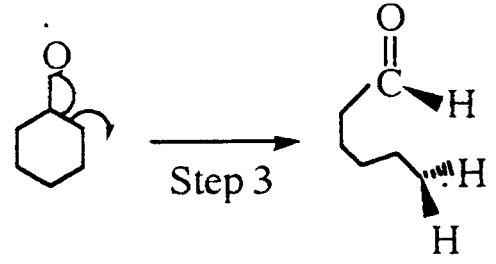

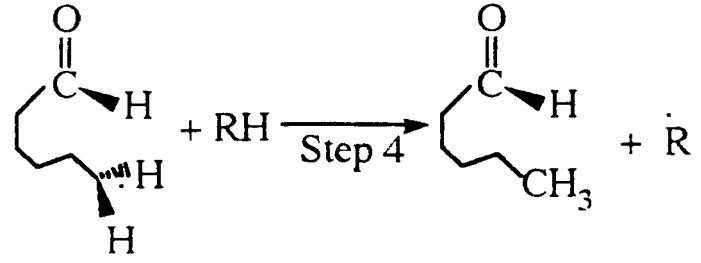

Scheme 5

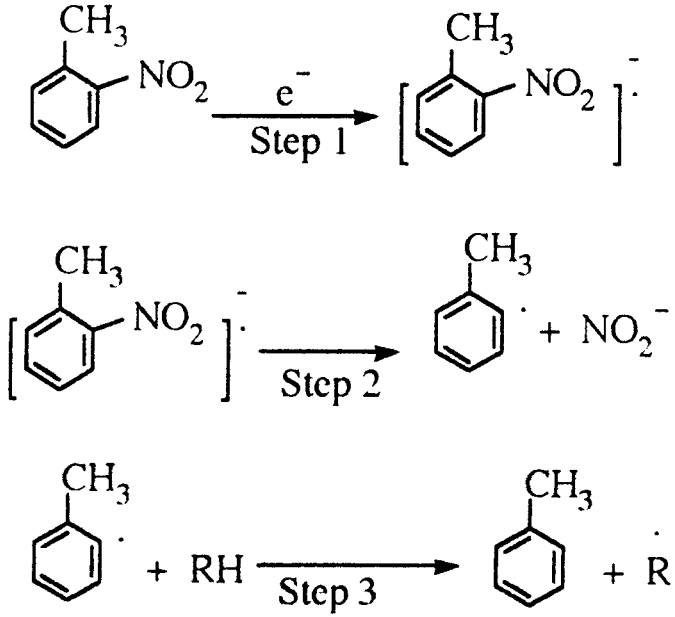

temperature. The sequence of reactions is shown below.

(9) $C_6H_5N_2^+ \rightarrow C_6H_5^+ + N_2$

$C_6H_5^+ + BF_4^- \rightarrow C_6H_5F + BF_3$

Benzenediazonium fluoroborate was pyrolyzed with methane using an initial pressure of 2.22 atm and 100 μs reaction time to obtain the data plotted in Figure1. A threshold value of 140 bar was found. It is desired to compare the peak temperature of methane at the threshold to the Arrhenius temperature at 100 μs relaxation time (k^{-1}). The compression ratio is calculated and used in equation (2) to find the temperature. Thus,

$$140 = 4.146\ (2.22)(V_o/V)^{1.24}\text{, so that}$$

$$T = 298(8.966)^{0.241} = 506\ K.$$

The pre-exponential factor, A, and activation energy of the Arrhenius equation for the decomposition of the related salt, p-tolydiazonium hydrogen sulfate, are calculated to be 7.5×10^{14} and 27760 cal/mole respectively from the data presented below[11].

T (°C)	$k \times 10^5$
0.03	0.960
9.94	4.11
69.93	15.7

Substitution of the A constant and the activation energy into the Arrhenius equation, with a relaxation time of 100 μs, gives a temperature of 554 K which agrees with the temperature at the threshold within the limits of uncertainty. Thus in the case of benzenediazonium salts, the temperature of the adiabatically compressed gas is nearly identical to the temperature of the reacting substate.

Figure 1

Benzenediazonium fluoroborate

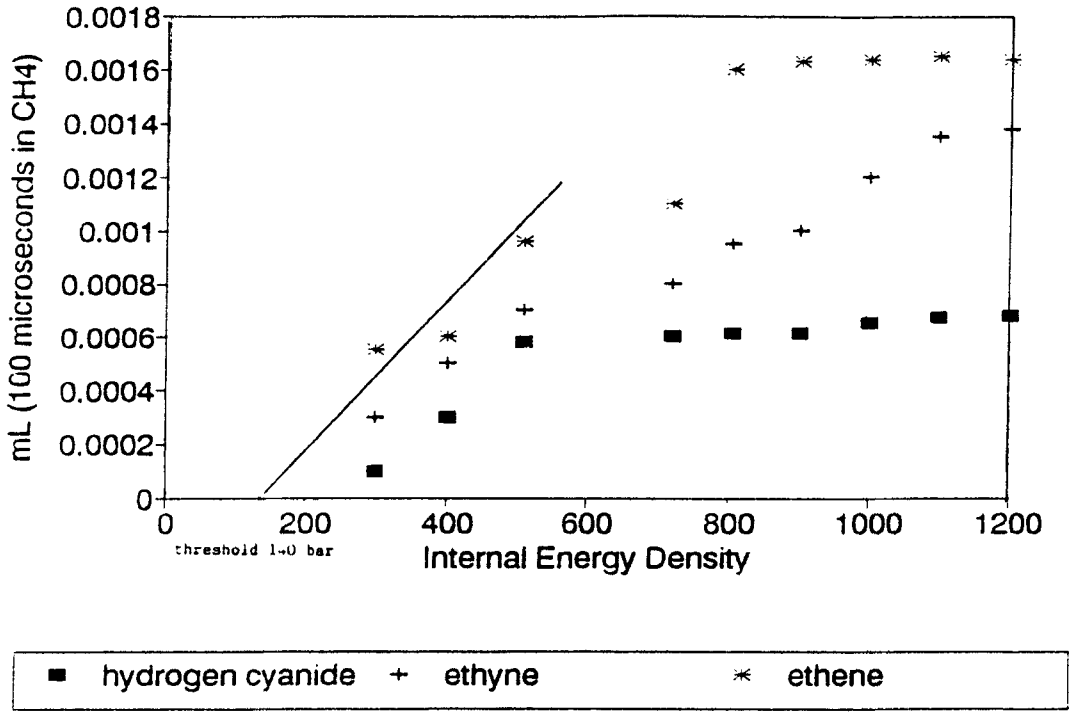

Figure 2

4-carboxybenzenediazonium salt

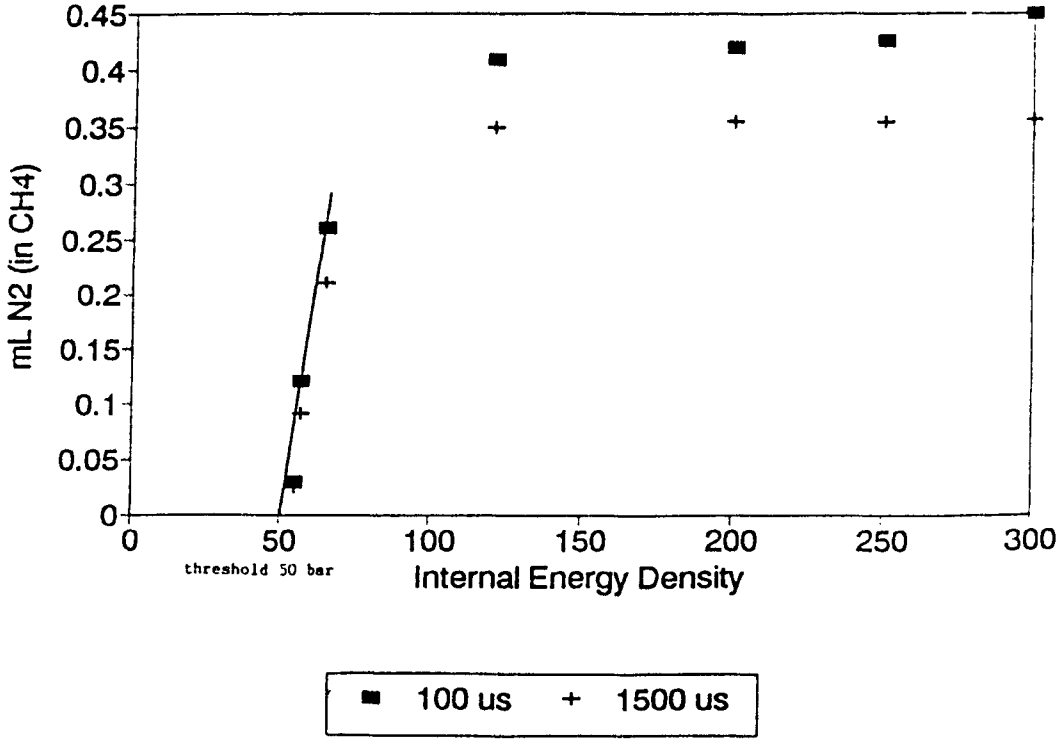

The steep gradient of the plots of mL of N_2 versus the internal energy density for the benzenediazonium salts attests to the absence of endothermic steps beyond the initial bond breaking. As shown in Figure 2 for the pyrolysis of 4-carboxybenzenediazonium chloride, once the threshold is exceeded, the reaction appears to go quickly to completion since there is little significant increase in N_2 as the internal energy density is increased from 100 to 300 bar.

Nitrate Esters

For plots such as those presented in Figure 3 for the pyrolysis of nitroglycerin, where NO/CO_x is plotted versus CO_x, there is a striking separation between plots at low values of CO_x. The NO/CO_x value falling on a vertical line at a constant value of CO_x can be multiplied by that quantity of CO_x to obtain the quantity of NO. The rate of consumption of NO can be inferred from the three values of NO/CO_x at the three reaction times for a particular value of CO_x. It is assumed that the reaction mixture will have had the same initial composition if the value of CO_x is the same because even at 100μs the consumption of NO is nearly complete. The reactive components of the fuel include organic radicals, CH_2O, HCN, C_2H_2, and H_2, in addition to CO which is the major component at the times in question.

During the pyrolysis of nitroglycerin, a state is reached where most of the unreduced nitrogen and oxidizable carbon take the form of NO and CO. At completion, nitrogen and carbon are converted to N_2 and CO_2. Even at the shortest reaction time of 100 μs, NO_2 has already been almost entirely converted to NO. From Figure 3, it is seen that NO represents 29% of the group, NO + CO + CO_2 after 100 μs reaction time at a small extent of pyrolysis. However, when pyrolysis is more extensive, the reduction of

NO is almost complete at 100 μs. We believe that thermal runaway is responsible for the rapid escalation in -d[NO]/dt and that thermal runaway is associated with good oxygen balance such as occurs in nitroglycerin and other highly energetic nitrate esters. For the nitroaromatics, on the other hand, these effects are less pronounced since the resulting reaction mixtures are oxygen deficient.

The decrease in NO/CO_x with CO_x for nitroglycerin pyrolysis is greatest at 100 μs. The fuel present at 100 μs (CO,CH_2O, C_2H_2 and others) along with NO gives a second order rate of disappearance of NO which is greatest at 100 μs since greater concentrations are present.

Nitramines

As for the nitrate esters, the nitramines gave lower quantities of NO when pyrolyzed at longer exposure times at a given value of internal energy density. When the transfer and analysis of the gas was strictly anaerobic, NO_2 was not observed even though NO_2 is produced initially from homolysis of the N-N bond of the nitramine group. The reason NO_2 is not observed is that reduction to NO and other products occurs before the reactions can be quenched.

One of the most interesting aspects of nitramine pyrolysis is the observation of N_2O at levels not usually found in the pyrolysates of other classes of compounds. For example, pyrolysis of 1,3-dinitro-1,2,3,4-tetrahydroimidazole gave levels of N_2O nearly equal to those of those of NO. The pyrolysis of 1-nitropyrrolidine, however, showed a low level of N_2O. The threshold of 1,3-dinitro-1,2,3,4-tetrahydroimidazole was found to be 200 bar and that of 1-nitropyrrolidine 305 bar (Figure 4).

It was found that RDX and HMX gave N_2O levels about equal to those of NO with thresholds of 240 and 327 bar respectively. It is tempting to

Figure 3
Nitroglycerin

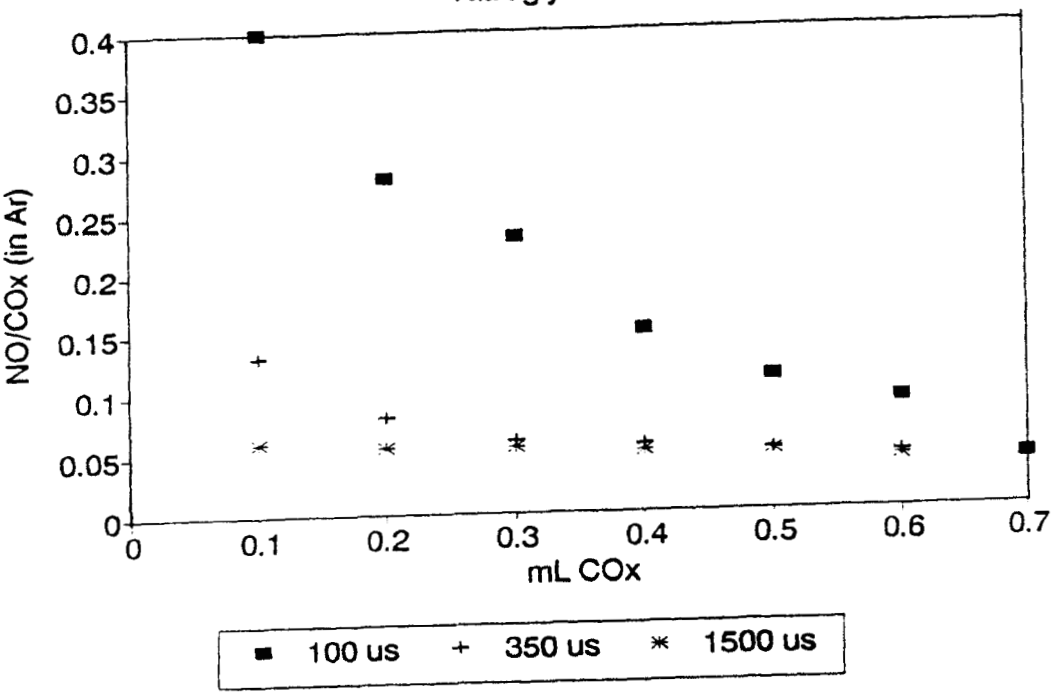

Figure 4

C4H8N2O2 (I) and C3H6N4O4 (II)

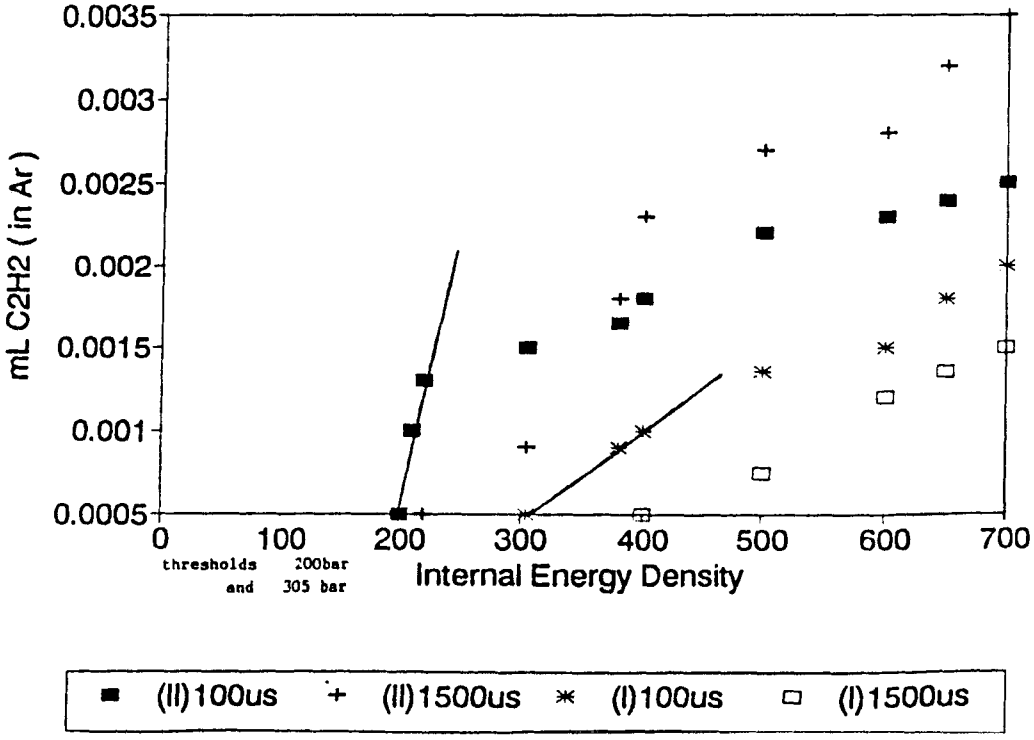

attribute the lower RDX threshold value of RDX to C-N bond weakening because of the greater ring strain of RDX. For HMX, Shaw and Walker[12] have pointed out that nine possible initial thermal decomposition steps are possible. Of the nine steps, three involve N-N bond breaking to produce NO_2, HONO, and HNO_2. The remaining possibilities all involve C-N bond breaking. There is therefore experimental evidence to substantiate both N-N and C-N bond breaking during the initial step of nitramine pyrolysis. As a final note, it should be emphasized that Behrens[13] work involving isotopic scrambling to support C-N bond breaking was performed at much lower temperatures and pressures than those of the present study. The point is that the pyrolysis mechanisms may well be different at higher temperatures and pressures.

Nitroaromatics

As for the nitrate esters and nitramines, the ratio of NO/CO_X was found to be greater at the shorter reaction times for all values COx for the pyrolysis of TNR, TNT, nitrobenzene, TATB, and trinitrobenzene. As discussed under the section for the nitrate esters, the vertical spacing of plots of NO/CO_X versus COx at the three reaction times is a reflection of the rate of consumption of NO. In Figure 5 it is seen that the values of NO/CO_X are greater for TNT than for TNR at all values of COx and at all reaction times. This means that the rate of disappearance of NO is less for TNT since the levels of NO/CO_X remain relatively high. On the other hand, NO has reacted extensively in the case of TNR since the levels of NO/CO_X are low. The reason TNR has a higher rate of consumption of NO is that TNR has a much better oxygen balance than TNT.

Figure 5
TNT and TNR

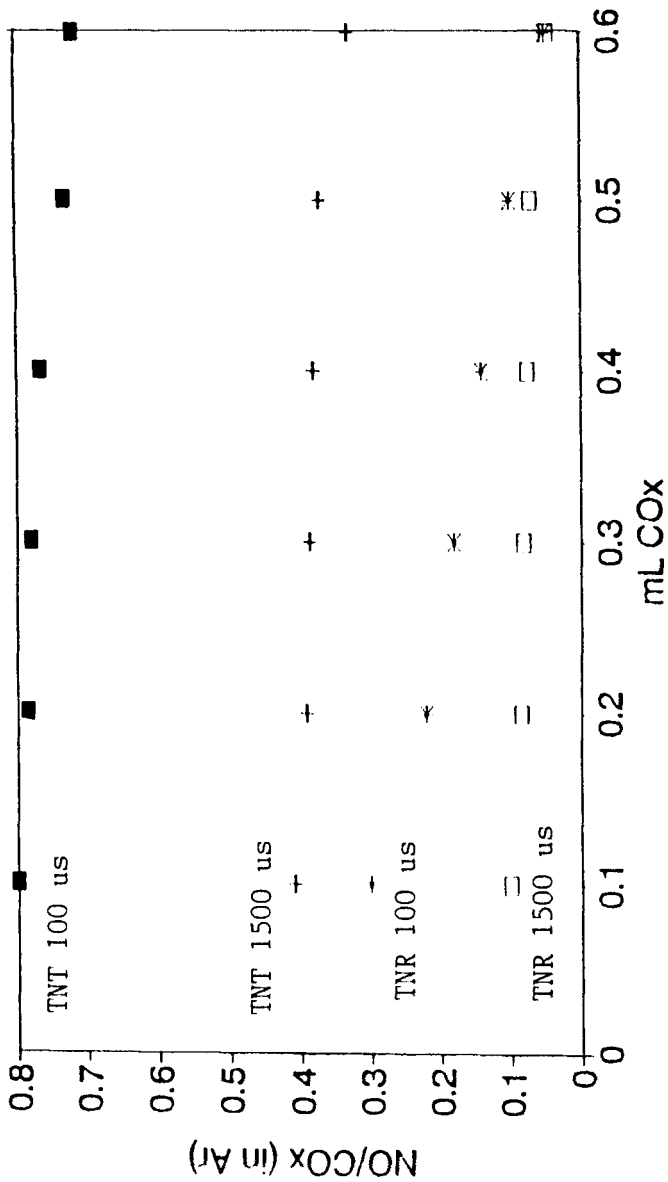

Figure 6

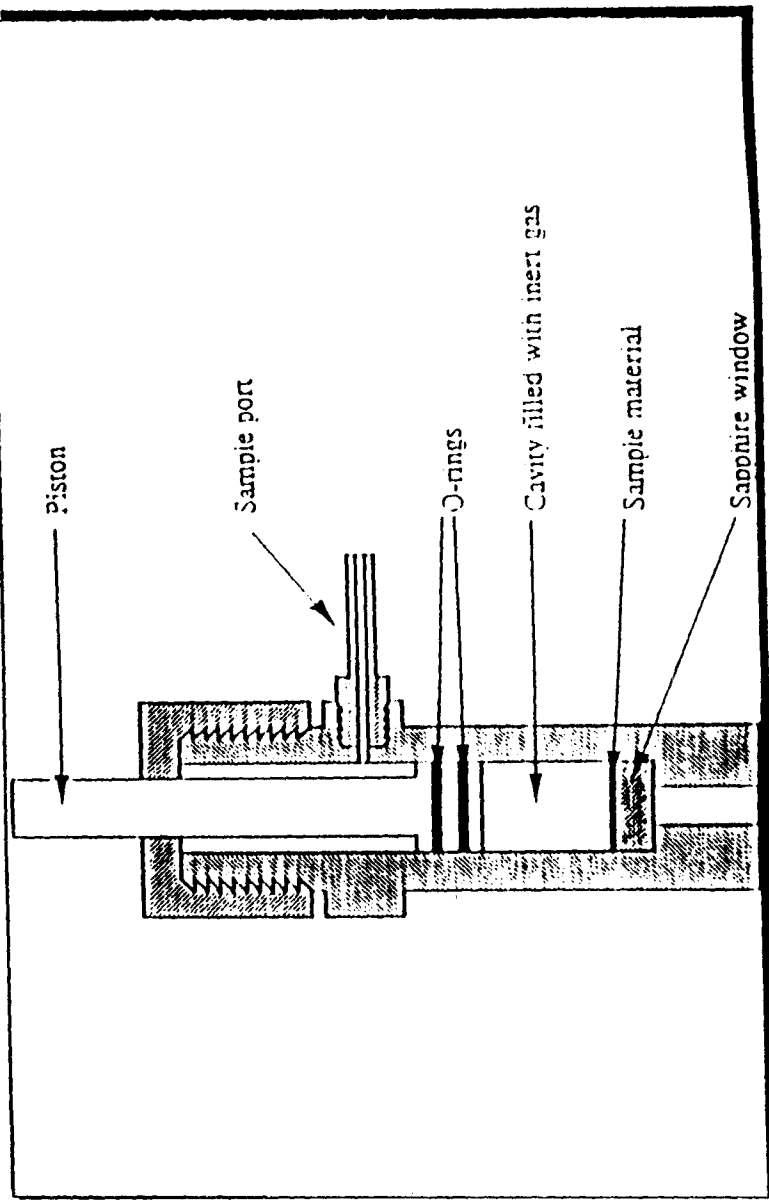

EXPERIMENTAL

Apparatus

All the pyrolyses were performed within the gas compression cell depicted in Figure 6 except that the apparatus for the shortest reaction time (100μs) has the emergent stem cut off just above the "o" rings . A 1.11 cm thick sapphire window aperture of 0.56 cm is located at the bottom of the cell. The piston is usually loaded with 10.0 mg of sample along with a 2.5 mm lead shot pellet which is partially flattened by the piston. Its thickness indicates the peak compression ratio.

The compression ratio, V_o/V, can be calculated using the expression,

$$V_o/V = \frac{5000}{127(S)25.4 - 11(mm)^3} \quad (10)$$

where,

S = shot thickness in inches

$V = \pi r^2 S$ - volume of lead shot $(mm)^3$

V_o = cavity volume in $(mm)^3$

The sidearm is maintained closed during the pyrolysis but later opened to allow the escape of gases to be analyzed by FTIR. For each trial, the piston cavity is evacuated with a vacuum pump andcharged with inert gas.

Three different reaction times of 1500 , 350 and 100 μs are used. The 1500 μs assembly is driven by a 2.8 kg dropweight and has a displacement transducer attached to a piston rod in the form of a knife edge which intersects a collimated light beam. The 2.8 kg dropweight is raised to a height up to 80-90 cm and released to impact the piston shaft stem. The 350 μs assembly is driven by a 100g pneumatic hammer located inside a barrel aligned with the piston shaft. The hammer is driven by

firing a wax-sealed cartridge loaded with up to 35 mg of smokeless powder. For the 100μs assembly , a 10.0g piston with no stem is impacted with a .22 bullet (long rifle, short or Cee Bee). A permanent magnet is embedded in the stainless steel 10.0g piston and an induction coil is on the outside of the cylinder to form a velocity transducer. The optical displacement transducer for the dropweight and hammer assemblies cannot be used because the piston has no stem.

A Fisher GC Series 2400 gas chromatograph , fitted with a column containing molecular sieve absorbant, is used to analyze for H_2 , N_2 , CO and CH_4.

A Perkin Elmer 1700 Series FTIR was used to analyze the gaseous pyrolysates withdrawn from the gas compression cell. The cell has a path length of 15.0 cm and a volume of 15.0 cm^3. Conversion of absorbance (A) to volume in mL , for absorbance values below 0.100 , was obtained using the data presented below.

COMPOUND	v (cm^{-1})	mL
CH_4	3017	A/6.1
CO_2	2360	A/7 0
CO	2169	A/1.0
NO	1903	A/1.0
NO_2	1629	A/5.8
N_2O	1298	A/1.5
N_2O	2236	A/7.0
C_2H_4	950	A/5.7
C_2H_2	730	A/23.0
HCN	713	A/10.0

A Hewlett-Packard 5890 GC with a 5970 Series Mass Selective Detector was used to obtain the ion chromatograms of the condensed phase residues remaining on the sapphire window of the cylinder. The residue was taken up with about 50.0 uL of methanol and transferred to a glass bulb for centrifugation and from 1.0 to 2.0 uL of clear liquid was then injected into the *GC-MS* port.

Data for Estimation of Surface Temperature

Three chemically stable salts with widely spaced melting points (KNO_3 334°C , $Ba(NO_3)_2$ 592 °C , and NaCl 802 °C) were subjected to heating by adiabatic compression at exposure times of 100 , 350 and 1500μs using compression ratios ranging from 20.0 to 65.0 at initial pressures ranging from 1.716 to 3.037 atm.

A 10.0 mg sample of crushed salt is evenly distributed on a thin glass slip within the cylinder and heated by adiabatic compression. Particles up to a certain maximum size are melted and form spheroidal beads. The diameter of the largest beads is measured with a filar micrometer on a microscope.

Procedure for Estimation of Gas Temperature

Equations (1) and (2) can be used to find the gas temperature for argon. For polyatomic gases, the equation of state,

$$(11) \qquad \int_{T_o}^{T_f} \frac{C_v\, dT}{T} = -\int_{V_o}^{V_f} \frac{R\, dV}{V} \quad ,$$

cannot readily be integrated because C_v becomes a function of temperature. We have developed the following procedure to calculate the temperature of polyatomic gases ,

(a) The temperature interval is divided into n subintervals for which C_v

becomes measured and calculated.

(b) The nth root of V_o/V is used in equation (1).

(c) Using the γ corresponding to the initial temperature , T_o, equation (1) is solved for T_1.

(d) The temperature , T_1 , found in step (c) serves as the initial temperature for the second subinterval. The γ corresponding to T_1 is used to calculate a temperature,T_2 , using equation (1).

(θ) Steps (c) and (d) are repeated a total of n times to arrive at the desired final temperature.

Preparation of Materials

Benzenediazonium fluoroborate and benzenedlazonlum perchlorate were prepared by first mixing 0.01 mole of aniline in 5.0 mL H_20 with 0.02 mole of HBF_4 ($B(OH)_3$ + 4 HF = HBF_4 + 3 H_20) or $HClO_4$ respectively, and then quickly adding 0.02 mole of $NaNO_2$ previously dissolved in 5.0 mL of H_20. The solids which formed were immediately suction-filtered and placed in a desiccator. Diazotized sulfanilic acid and 4-carboxybenzenediazonium chloride were prepared by mixing 0.01 mole of sulfanilic acid or 0.01 mole of para-aminobenzoic acid, respectively, with 0.02 mole of HCl dissolved in 5.0 mL of H_20 and then quickly adding 0.02 mole of $NaNO_2$ previously dissolved in 5.0 mL of H_20.

Cyclohexanol nitrate, 1,2-propanediol dinitrate and ethyleneglycol dinitrate were prepared according to Soffer, Parotta and DiDomenico[14] and Weygand[15].

The nitramines, 1-nitropyrrolidine and 1,3-dinitro-1,2,3,4-tetrahydroimidazole were prepared by first forming the nitrate (neutralizing the amine with 70% HNO_3 and evaporating to dryness under

20 mm pressure). To 0.034 mole of the nitrate and 0.0017 mole of anhydrous $ZnCl_2$ is added 0.098 mole of acetic anhydride and the mixture stirred at 60 °C for 30 minutes, cooled, and then neutralized with aqueous alkali. After extraction with diethylether and extraction of the ether with 10% H_2SO_4, the ether layer is dried with $CaCl_2$, filtered and evaporated to give the crude nitramine which is recrystallized with absolute ethanol.

N-nitropiperidine was prepared as described above but the evaporation of ether resulted in a crude oil which contained N-nitrosopiperidine as an impurity. The crude oil was eluted through a silica gel column with petroleum ether and the first fractions collected contained only N-nitropiperidine.

The nitroaromatics, trinitroresorcinol (TNR), nitrobenzene (NB), trinitrotoluene (TNT), trinitrobenzene (TNB), and triaminotrinitrobenzene (TATB) were synthesized as described by Davis[16]. Deuterated orthonitrotoluene was prepared according to Hickinbottom[17] using d_8 - toluene and β - nitrostyrene was purchased from Aldrich.

REFERENCES

(1) Bowden,F.P. and Gurton,O.A. Proc. Roy. Soc. A., 198, 337, (1949).

(2) Evans,J.I. and Yuill,A.M. Proc. Roy. Soc. A., 246, 176, (1950).

(3) Friedman, M.H. Combust. Flame , 11(3), 239, (1967).

(4) Rice,O.K. J. Chem. Phys., 8, 727, (1940).

(5) Taylor, J.W. Trans. Faraday Soc., 58, 561, (1962) .

(6) Hicks, B. L. J. Chem. Phys., 22, 414, (1954).

(7) Pasman, H.J Chem. Prob. Connected Stab. Explosives (Proc.) 3rd,180, (1974).

(8) Brower, K.R. Sixteenth International Pyrotechnics Seminar, Sweden, 185, (1991).

(9) Cohn, R.H. Ph.D. Thesis , Thermal Decomposition of Nitromethane by Adiabatic Gas Compression, New Mexico Institute of Mining and Technology, (1990)

(10) Montanari, S., Paradisi,C. and Scorrano, G. J. Org. Chem., 58, 5628, (1993).

(11) Taylor, J.E. and Feltis, T.J. J. Amer. Chem. Soc., 74, 1331, (1952).

(12) Shaw, R. and Walker, F.E. J. Phys. Chem., 81, 2572, (1977).

(13) Behrens, R. J. Phys. Chem., 94, 6706, (1990).

(14) Soffer, L.M.,Parotta,E.W. and Di Domenico, J. J. Amer. Chem. Soc., 74, 5302, (1952).

(15) Weygand,C. *Organic Preparations* , Interscience Publishers,NY,280, (1945).

(16) Davis,T.L. *The Chemistry of Powders and Explosives* , Angriff Press,CA,125.

(17) Hickinbottom,W.J. *Reactions of Organic Chemistry*, Longmans and Green ,48, (1948).